Structures of (3*n*-crown-*n*)-Phenol (*n*=4, 5, 6, 8) Host-Guest Complexes: Formation of a Uniquely Stable Complex for *n*=6 via Collective Intermolecular Interaction

Ryoji Kusaka, Yoshiya Inokuchi, Takeharu Haino and Takayuki Ebata*

Department of Chemistry, Graduate School of Science, Hiroshima University, Higashi-Hiroshima 739-8526, Japan

Abstract

Structures of crown-phenol 1:1 host-guest complexes, 3*n*-crown-*n* [12C4(*n*=4), 15C5(*n*=5), 18C6(*n*=6), 24C8(*n*=8)], in the gas phase have been studied by various laser spectroscopic methods. The S_1-S_0 electronic spectra identified 3, 2, 1, and 2 isomers for the complexes of 12C4, 15C5, 18C6, and 24C8, respectively, suggesting that only 18C6-phenol forms one uniquely stable complex. The IR spectra in the phenolic OH and CH stretch regions indicate that these complexes form the O•••HO hydrogen bond and the benzene ring is involved in the complex formation. Theoretical analysis with molecular mechanics and density functional theory calculations also supports one considerably stable isomer for 18C6-phenol. The most stable 18C6-phenol isomer is largely stabilized through collective intermolecular interaction consisting of O•••HO hydrogen bond, CH•••π, and O•••HC(aromatic) so that phenol is inserted into the cavity of a particular conformation of 18C6 like a "**lock and key**".

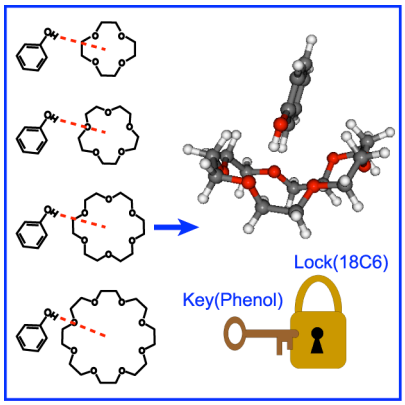

TOC graphic

Key word: phenol, crown ethers, host-guest complex, molecular recognition, lock and key

Since Pedersen discovered crown (macrocyclic) ethers (CEs) in 1967[1,2], a number of studies on CEs have been reported as models of bio-receptors[3]. Generally it is well known that the binding efficiency of CEs is highly dependent on their sizes, and a CE effectively binds a guest species when the size of the guest is reasonably matched with that of the CE cavity. However, the mechanism of the complexation is not so simple because CEs are generally so flexible that they can adjust their conformations to the shape of a guest, which is called induced-fit[3]. For example, it has been reported that dibenzo-24-crown-8, dibenzo-30-crown-10 and 30-crown-10 wrap a K^+ cation by folding their large and flexible CE rings[3]. Furthermore, very recently we reported that dibenzo-18-crown-6 and benzo-18-crown-6 effectively capture an H_2O or an NH_3 molecule by adjusting their flexible conformations[4,5]. In this paper, we investigated structures of CE-phenol 1:1 complexes in a supersonic jet. For CEs, a series of 3*n*-crown-*n* shown in Figure 1 [12C4(*n* = 4), 15C5(*n*=5), 18C6(*n*=6), 24C8(*n*=8)] was selected to study how the size of 3*n*C*n* influences the structures of the complexes.

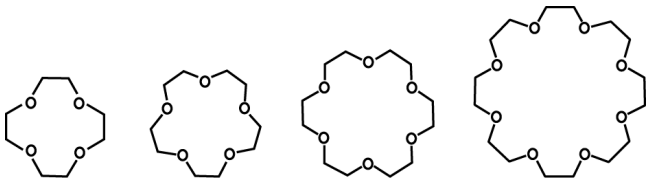

Figure 1. Crown ethers (3*n*C*n*, *n* = 4, 5, 6 and 8)

As we shall see, the 3*n*C*n*-phenol complexes are formed through multiple intermolecular interactions such as O•••HO hydrogen(H)-bond, CH•••π, and O•••HC(aromatic), so that we also study how the multiple interactions change with the size of 3*n*C*n*. We apply variety of laser spectroscopic methods to the structural investigation of the jet-cooled 3*n*C*n*-phenol complexes. The S_1-S_0 electronic spectra are measured by laser induced fluorescence (LIF) spectroscopy, and the discrimination of isomers is performed by UV-UV hole burning (UV-UV HB) spectroscopy. IR spectra in the OH and CH stretching region are measured by IR-UV double-resonance (IR-UV DR)

spectroscopy. We also examine diethyl ether (DEE)-phenol and 1,4-dioxane (DO)-phenol complexes to compare them with the 3*n*C*n*-phenol complexes. The experimental results are analyzed with the aid of theoretical calculations.

Figure 2(a) shows an LIF spectrum of phenol-H_2O[6] and $(phenol)_2$[7] in the S_1-S_0 band origin region. Figures 2(b)-(g) are LIF spectra of DEE-phenol[8], DO-phenol[8], and 3*n*C*n*-phenol (*n* = 4, 5, 6 and 8) complexes, respectively. As seen in the spectra, each complex shows sharp vibronic structures. Very weak bands in the region of 35600-35800 cm^{-1} for 12C4 [Figure 2(d)] and 18C6 [Figure 2(f)] are assigned to the 12C4-$(phenol)_{2\text{-}3}$ and 18C6-$(phenol)_{2\text{-}3}$ complexes, respectively, because their IR-UV DR spectra show more than one H-bonded OH stretching bands with comparable intensity, although the spectra are not shown here. The LIF spectrum of 24C8-phenol [Figure 2(g)] shows broad background beneath the sharp vibronic bands. This broad electronic transition may be due to larger complexes and minor 1:1 complexes.

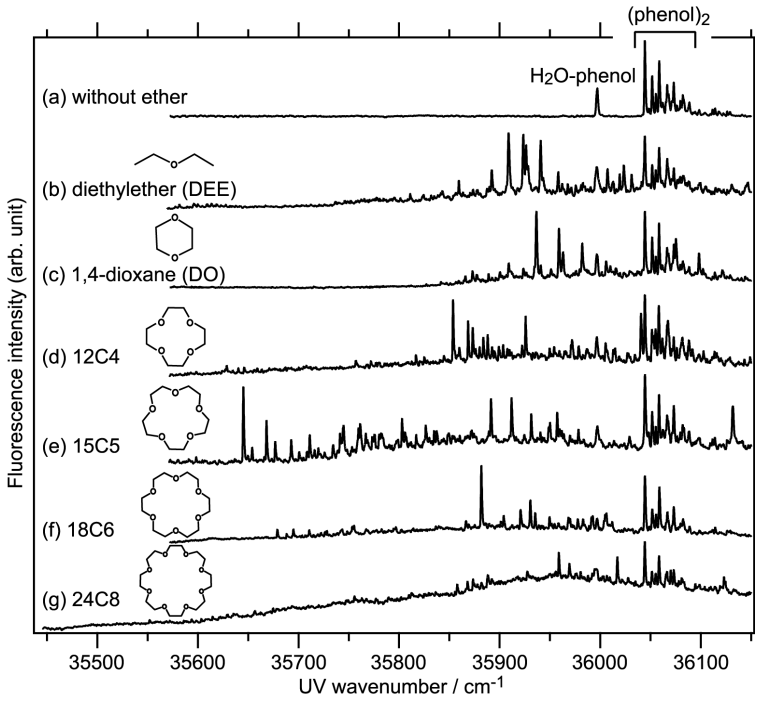

Figure 2. LIF spectra of (a) H_2O-phenol, $(phenol)_2$, and (b)-(g) ether-phenol complexes.

Figure 3 shows the LIF and UV-UV HB spectra of the DEE-phenol, DO-phenol and

3*n*C*n*-phenol complexes. The UV-UV HB spectra were measured by fixing probe laser frequencies to vibronic bands having large intensity in the LIF spectra. As seen in the spectra, the UV-UV HB spectra reproduce almost all the bands in the LIF spectra. We could indentify 1, 1, 3, 2, 1, and 2 isomers for the complexes of DEE, DO, 12C4, 15C5, 18C6, and 24C8 complexes, respectively. For the 24C8-phenol complex [Figure 3(f)], we also measured UV-UV HB spectra of the broad background by fixing probe laser frequencies to positions near bands A and B (green curves). Both green spectra reproduce well the broad background signal in the LIF spectrum. The positions of the origin bands of the complexes are listed in Table 1.

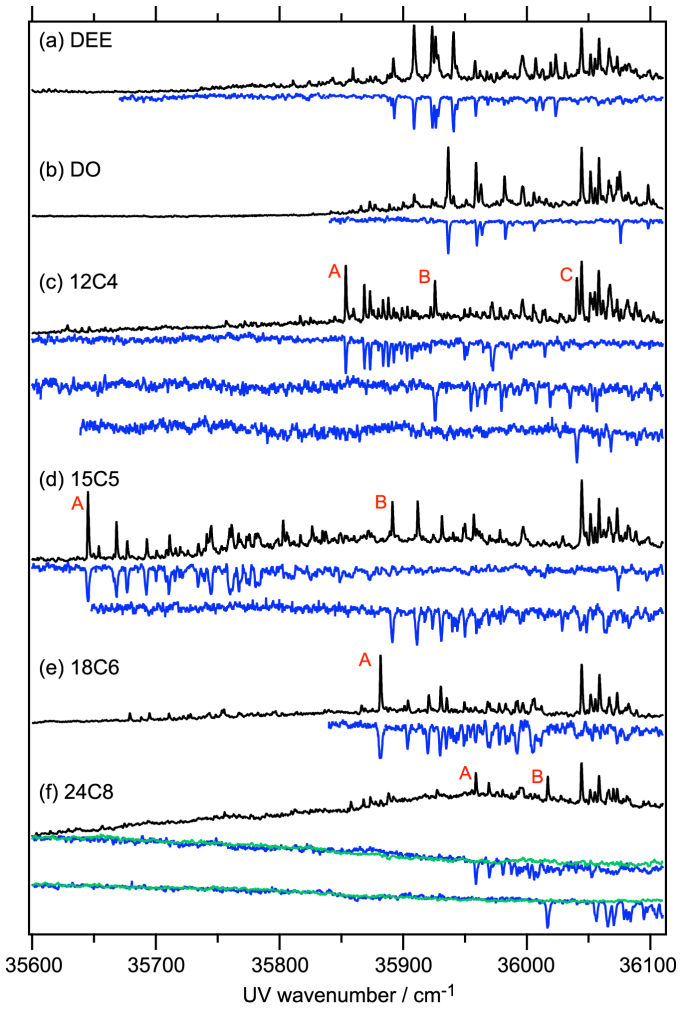

Figure 3. LIF (black) and UV-UV HB (blue and green) spectra of ether–phenol complexes. Green spectra for 24C8 were obtained by fixing probe UV frequency to positions near bands A and B.

Table 1 Positions of S_1-S_0 origin bands, and OH stretching vibrational frequencies of the H-bonded complexes of phenol. The value of red shift relative to bare phenol is shown in parentheses.

Species	Band origin / cm^{-1}	OH stretching frequency/ cm^{-1}
phenol	36348	3657
$(phenol)_2$	36044 (304)	3530(127), 3655(2)[a]
phenol-H_2O	35997 (351)	3522 (135)
phenol-DEE	35888 (460)	3367 (290)
phenol-DO	35937 (411)	3387 (270)
12C4(A)	35854 (494)	3344 (313)
12C4(B)	35926 (422)	3426 (231)
12C4(C)	36040 (308)	3389 (268)
15C5(A)	35645 (703)	3411 (246)
15C5(B)	35891 (457)	3338 (319)
18C6(A)	35882 (466)	3431 (226)
24C8(A)	35959 (389)	3427 (230)
24C8(B)	36017 (331)	3454 (203)

a) OH of the H-bond acceptor .

Figure 4 shows IR-UV DR spectra of (a) bare phenol, (b) $(phenol)_2$, (c) phenol-H_2O, and (d)-(m) 3*n*C*n*-phenol complexes. The bands in the 3300-3700 and 3000-3100 cm^{-1} region are due to phenolic OH and CH stretching vibrations, respectively, and those in the 2800-3000 cm^{-1} region are the methylene CH stretching vibrations of ethers. For 24C8-phenol [Figures 4(l) and (m)], the IR-UV DR spectra measured by monitoring the broad transition are also shown as green spectra. In Figures 4(b)-(m), the OH stretching bands are red-shifted by 100-300 cm^{-1} from that of bare phenol [3657 cm^{-1}, Figure 4(a)], indicating that the phenolic OH group is H-bonded as a proton donor in all the complexes. All the H-bonded OH bands of the ether-phenol complexes [Figures 4(d)-(m)] are accompanied by low-frequency bands. These bands are the combination bands of the H-bonded OH stretch and intermolecular vibrational modes. Such combination bands are also observed in other complexes having strong H-bonds.[9,10]

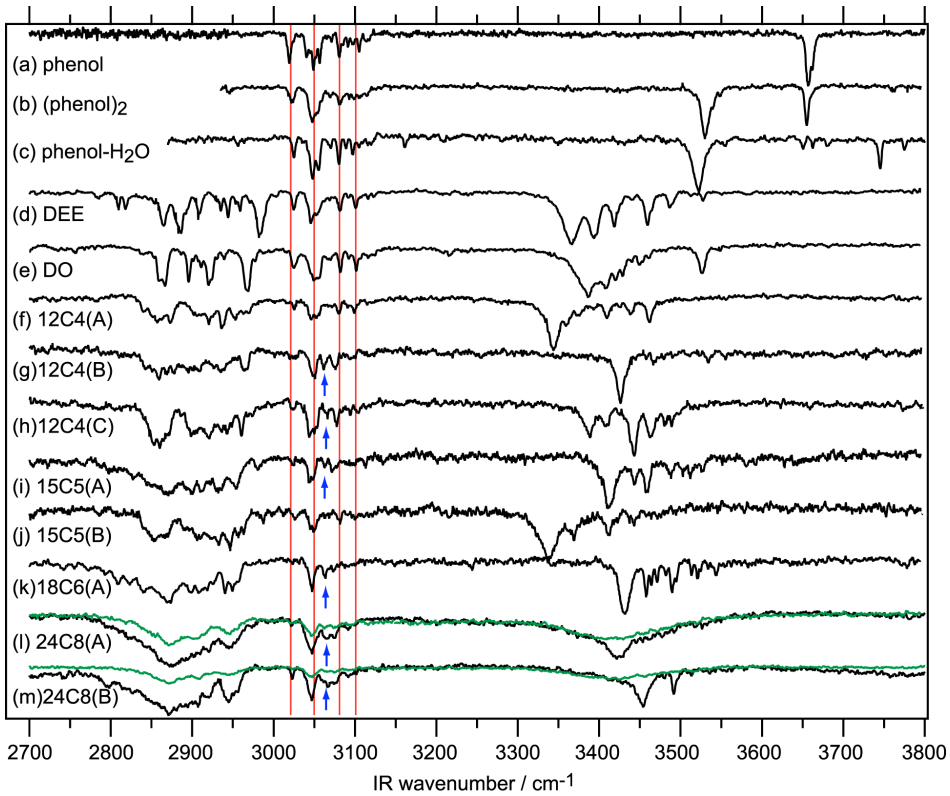

Figure 4. IR-UV DR spectra of (a) bare phenol, (b) $(phenol)_2$, (c) phenol-H_2O, and (d)-(m) ether-phenol complexes. Green spectra for 24C8 were obtained by fixing probe UV frequency to positions near bands A and B.

For aromatic CH stretch bands, they can be classified into four groups, ~3025, ~3050, ~3075, and ~3100 cm^{-1}, as highlighted by red lines in Figure 4. Among them, the intensities of the bands at ~3025, ~3075, and ~3100 cm^{-1} of the 3*n*C*n*-phenol complexes [Figure 4(f)-(m)] are weaker than those of bare phenol, $(phenol)_2$, phenol-H_2O, DEE-phenol, and DO-phenol [Figure 4(a)-(e)]. Furthermore, new bands appear in the 3050-3075 cm^{-1} region of almost all 3*n*C*n*-phenol complexes, as indicated by arrows. The spectral difference in the aromatic CH region from those of bare phenol, $(phenol)_2$, phenol-H_2O, DEE-phenol, and DO-phenol [Figures 4(a)-(e)] implies that the aromatic ring of phenol is involved in the formation of the 3*n*C*n*-phenol complexes. The spectral feature of methylene CH stretch is complicated and the bandwidths become broader with increasing the ether size.

As described above, we identified the number of major isomers for the complexes of 12C4,

15C5, 18C6, and 24C8 as 3, 2, 1, and 2, respectively, from the UV-UV HB spectra (Figure 3). From this result, we can propose that only the 18C6-phenol complex forms one uniquely stable complex but the other three complexes (12C4, 15C5, and 24C8) do not. Theoretical analysis supports the existence of one predominantly stable isomer for the 18C6-phenol complex. Table 2 lists relative total energies (ΔE / cm^{-1}) of the six lowest-energy 3*n*C*n*-phenol complexes (I-VI) optimized at ωB97X-D/6-31++G** level of theory. ΔE of the second stable isomers (II) of the 3*n*C*n*-phenol (*n*=4, 5, 8) complexes are 43, 16, and 124 cm^{-1}, respectively. On the other hand, that of the 18C6-phenol complex is 642 cm^{-1}, which is much larger than those of the other three complexes. Thus, the theoretical calculation predicts that 18C6-phenol has one uniquely stable isomer while the 3*n*C*n*-phenol (*n*=4, 5, 8) complexes do not.

Table 2 Relative total (ΔE) and intermolecular interaction (E_{int}) energies of the six most stable isomers of 3*n*C*n*-phenol 1:1 complexes optimized at ωB97X-D/6-31++G** level. ΔE(CE) is relative energy of the conformation of crown part in each complex. ΔG is relative Gibbs energy of a complex at 298.15 K and 1 atm. They are shown in cm^{-1} unit.

	12C4 (*n*=4)				15C5 (*n*=5)				18C6 (*n*=6)				24C8 (*n*=8)			
	ΔE	E_{int}	ΔE(CE)	ΔG	ΔE	E_{int}	ΔE(CE)	ΔG	ΔE	E_{int}	ΔE(CE)	ΔG	ΔE	E_{int}	ΔE(CE)	ΔG
I	0	5939	186	0	0	6872	507	381	0	8354	265	0	0	10157	1225	0
II	43	6007	303	87	16	7175	961	294	642	7965	351	812	124	9806	844	72
III	88	5859	124	171	74	6129	0	0	684	7710	179	552	419	9730	929	628
IV	99	5727	0	253	197	6447	283	583	872	7426	0	1047	586	8692	0	790
V	183	5963	333	277	220	7102	967	479	951	7352	134	736	623	9303	891	581
VI	280	5870	328	508	375	6304	331	596	991	7672	379	955	677	9240	863	592

In order to investigate the reason of the unique stability of 18C6(I)-phenol, we calculated intermolecular interaction energies (E_{int} / cm^{-1}, Table 2) by using Eq. (1) (See **Computational**). Among the 18C6-phenol isomers, 18C6(I)-phenol has much larger E_{int} (8354 cm^{-1}), suggesting that the lowest ΔE of the 18C6(I)-phenol isomer is mostly due to the strong intermolecular interaction.

On the other hand, the 12C4(II)-, 15C5(II)-, and 24C8(I)-phenol complexes have the largest E_{int} (6007, 7175, and 10157 cm^{-1}, respectively) among the isomers but their ΔE are not as low as those expected from their E_{int}. Table 2 also lists relative energies of the conformation of the crown part in each complex [ΔE(CE) / cm^{-1}]. ΔE(CE) of the 12C4(II), 15C5(II), and 24C8(I) conformations have relatively large energies (303, 961, and 1225 cm^{-1}, respectively) among the isomers, so ΔE of the 12C4(II)-, 15C5(II)-, and 24C8(I)-phenol isomers are not so low due to the instability of their crown conformations. Thus, it is concluded that not only a strong intermolecular interaction (E_{int}) but also the stability of crown conformation [ΔE(CE)] are essential for the unique stability of the 3*n*C*n*-phenol complexes. In the 18C6-phenol system, both factors facilitate the stabilization of the 18C6(I)-phenol isomer.

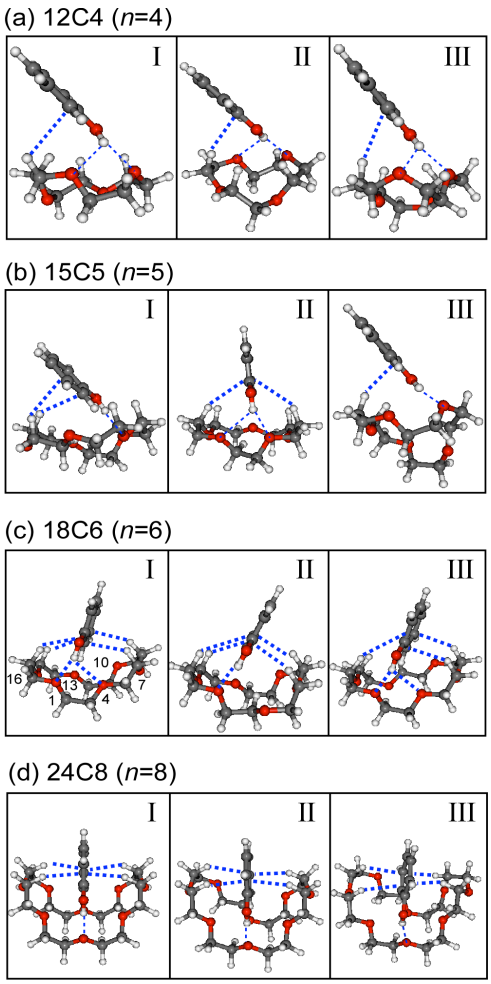

Figure 5. Three most stable isomers of each 3*n*C*n*-phenol complex optimized at the ωB97X-D/6-31++G** level.

Figure 5 shows the optimized structures of the three lowest-energy isomers of 3*n*C*n*-phenol (*n* = 4, 5, 6, and 8) complexes. Blue dotted lines represent the O•••HO H-bond ($\Delta r_{O\cdots H}$< 2.7 Å) and CH•••π interaction ($\Delta r_{H\cdots C}$ < 3.0 Å). In these complexes, the conformations of the crown part are different from each other, a phenolic OH is H-bonded to ether O atom(s), and its π electrons interact with the crown CH group(s). In most of the 12C4- and 15C5-phenol isomers [Figures 5(a) and (b)], phenol interacts with crown CHs at one side of the phenyl ring. On the other hand, in the 18C6- and 24C8-phenol complexes [Figures 5(c) and (d)], the phenyl ring is bound to crown CHs on both sides. Especially in the three 24C8-phenol isomers [Figure 5(d)], phenol is completely included in the 24C8 cavity via O•••HO H-bond and four CH•••π interactions, resulting in large E_{int} (Table 2).

The reason why only 18C6(I)-phenol has the much larger E_{int} among the isomers is described from the analysis of the conformation of 18C6 part. Figure 6 picks out the structures of the 18C6 part in the 18C6(I, II and III)-phenol complexes. In the 18C6(I) conformation [Figure 6(a)], four oxygen atoms, O(1) O(4) O(10) and O(13) are directed toward the inside of the cavity, so that a phenol molecule collectively interacts with the four O atoms via bifurcated [O(1)•••HO and O(4)•••HO] H-bonding, CH•••π, O(10)•••HC(aromatic), and O(13)•••HC(aromatic) interactions [Figure.5(c)]. On the other hand, the conformations of 18C6(II) [Figure 6(b)] and 18C6(III) [Figure 6(c)] are slightly different from that of 18C6(I) as represented by blue solid lines, namely -O(4)-C(3)-H(3) part for 18C6(II) and -O(13)-C(12)-H(12) part for 18C6(III). In 18C6(II), O(4) is directed toward the outside of the cavity and H(3) hinders phenol from forming the bifurcated O•••HO H-bond [Figure 5(c)]. Similarly in 18C6(III), O(13) is directed toward the outside of the cavity and H(12) hinders the O(13)•••HC(aromatic) interaction [Figure 5(c)]. These results imply that the shape of a phenol molecule is best matched into the cavity of 18C6(I) and the largest E_{int} of the 18C6(I)-phenol isomer is due to collective intermolecular interaction consisting of O•••HO, CH•••π and O•••HC(aromatic).

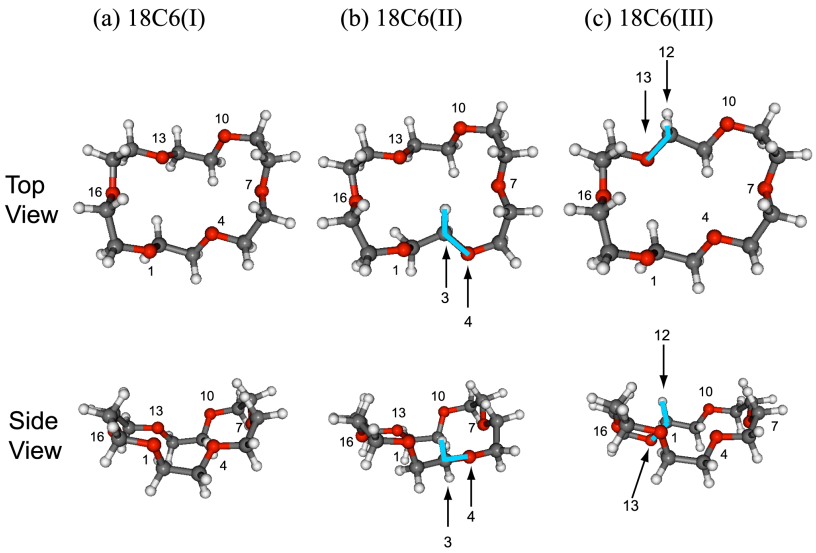

Figure 6. Conformations of 18C6 part in the three most stable 18C6-phenol complexes in Figure 5(c).

Table 2 also shows relative Gibbs energy (ΔG / cm^{-1}) at 298.15 K and 1 atm. ΔG of the second stable isomers of the 3*n*C*n*-phenol (*n*=4, 5, 8) complexes [12C4(II)-phenol, 15C5-(II)-phenol, and 24C8(II)-phenol] are 87, 294, 72 cm^{-1}, respectively, whereas that of the 18C6-phenol complex [18C6(III)-phenol, 552 cm^{-1}] is much larger than those of the other three complexes. Thus, the DFT calculation also predicts that the 18C6(I)-phenol isomer is uniquely stable in Gibbs energy and this isomer can dominantly exist even at room temperature.

Here we discuss whether the O•••HO H-bond is essential for the unique stability of the 18C6(I)-phenol complex by comparing the calculated results of 3*n*C*n*-phenol with those of 3*n*C*n*-benzene (*n*=4, 5, 6, 8) complexes. Geometrical optimizations of 3*n*C*n*-benzene (ωB97X-D/6-31++G**) were performed with initial geometries generated by replacing a phenolic OH group in the optimized 3*n*C*n*-phenol complexes with an H atom. The structures of the optimized 3*n*C*n*-benzene complexes (not shown) are very similar to those of the 3*n*C*n*-phenol complexes. Table 3 shows ΔE, E_{int}, ΔE(CE), and ΔG of the 3*n*C*n*-benzene complexes. As seen in the table, ΔE of the second stable isomers of 3*n*C*n*-benzene (*n*=4, 5, 8) complexes [12C4(V)-benzene, 15C5(I)-benzene, 24C8(IV)-benzene] are 33, 102, and 187 cm^{-1}, respectively. These energy gaps are much smaller than that of 18C6(II)-benzene complex, 362 cm^{-1}, suggesting that 18C6(I)-benzene retains the unique

stability. This result indicates that van der Waals interactions such as CH•••π and O•••HC(aromatic) are essential for the stabilization of 18C6(I)-phenol. However, the O•••HO H-bond also contributes to the unique stability of the 18C6(I)-phenol complex because Δ*E* of the second stable isomer is reduced from 642 cm^{-1} of 18C6(II)-phenol (Table 2) to 362 cm^{-1} of 18C6(II)-benzene (Table 3).

Table 3 Relative total (Δ*E*) and intermolecular interaction (E_{int}) energies of 3*n*C*n*-benzene 1:1 complexes optimized by using the 3*n*C*n*-phenol structures as initial geometries (ωB97X-D/6-31++G**). Δ*E*(CE) is relative energy of the conformation of crown part in each complex. Δ*G* is relative Gibbs energy of a complex at 298.15 K and 1 atm. They are shown in cm^{-1} unit.

	12C4 (*n*=4)				15C5 (*n*=5)				18C6 (*n*=6)				24C8 (*n*=8)			
	Δ*E*	E_{int}	Δ*E*(CE)	Δ*G*	Δ*E*	E_{int}	Δ*E*(CE)	Δ*G*	Δ*E*	E_{int}	Δ*E*(CE)	Δ*G*	Δ*E*	E_{int}	Δ*E*(CE)	Δ*G*
I	0	2810	3	0	102	3591	477	103	0	4816	193	0	0	6298	1156	0
II	166	2842	207	196	0	3910	872	0	362	4667	335	510	223	5873	668	600
III	46	2783	0	60	187	3029	0	319	421	4369	100	379	447	5873	861	893
IV	-[a]	-[a]	-[a]	-[a]	120	3461	353	298	777	3871	0	845	187	5378	0	820
V	33	3116	325	5	584	3351	806	781	773	4081	146	772	273	5885	691	741
VI	-[b]	-[b]	-[b]	-[b]	171	3450	397	483	-[c]	-[c]	-[c]	-[c]	359	5770	642	654

[a] 12C4(IV)-benzene structure is the same as 12C4(III)-benzene one.

[b] 12C4(VI)-benzene structure is the same as 12C4(V)-benzene one.

[c] 18C6(VI)-benzene structure is the same as 18C6(II)-benzene one.

Finally, we discuss the large red shift of S_1-S_0 electronic transition of 15C5(A)-phenol complex (Figure 3). As seen in the electronic spectra of Figure 3, the S_1-S_0 electronic transition energy of 15C5(A)-phenol is much lower than those of the other complexes. The red-shift of the S_1-S_0 origin of 15C5(A)-phenol is 703 cm^{-1} from that of bare phenol while those of the other complexes are 300-500 cm^{-1} (Table 1). This large red-shift of 15C5(A)-phenol may suggest a strong O•••HO H-bond of this complex because in general the S_1-S_0 transition energy of H-bonded complex of phenol becomes lower with the strength of the H-bond[11]. However, as seen in Figure 4 and Table 1, the frequency of H-bonded OH stretching frequency of 15C5(A)-phenol complex (3411 cm^{-1}) is

not so different from those of the other complexes, suggesting that the large red-shift of 15C5(A)-phenol cannot be attributed simply to a substantially strong O•••HO H-bond.

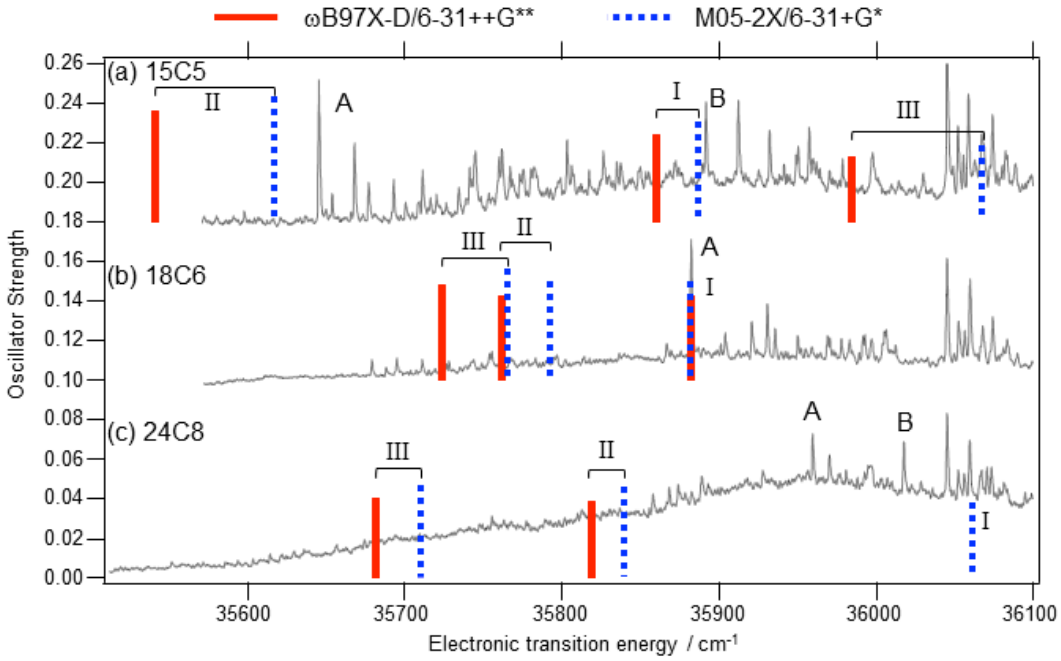

Figure 7. Comparison between LIF spectra and vertical calculated S_1-S_0 electronic transition energies for (a) 15C5-phenol, (b) 18C6-phenol, and (c) 24C8-phenol, calculated with TD-DFT at the ωB97X-D/6-31+G** (solid bar) and M05-2X/6-31+G* (dotted bar) levels. The calculated transition energies are scaled by a factor of 0.86596 for ωB97X-D/6-31+G** and 0.84143 for M05-2X/6-31+G* so that the transition energy of 18C6(I)-phenol reproduces the band origin of 18C6(A)-phenol. The calculated transition energy and the oscillator strength of 24C8(I)-phenol at the ωB97X-D/6-31+G** level are not shown because of their anomalous, unreliable values [40941 cm^{-1} (scaled) and 0.0018, respectively]

The results of the time-dependent DFT (TD-DFT) calculation reproduce the large red-shift of 15C5(A)-phenol. Figure 7 shows the comparison of the observed LIF spectra of crown-phenol complexes and the S_1-S_0 transition energies for 15C5(*n*)-phenol, 18C6(*n*)-phenol and 24C8(*n*)-phenol complexes with *n* = I ~ III, obtained by TD-DFT calculation at M05-2X/6-31+G* and ωB97X-D/6-31++G** levels. The calculated S_1-S_0 transition energies are scaled so that the transition energy of the most stable isomer of 18C6(I)-phenol fits to the origin band of

18C6(A)-phenol. It is seen that one of the three stable 15C5-phenol isomers, that is 15C5(II)-phenol, shows a largely red-shifted electronic transition, indicating that 15C5(II)-phenol can be assigned to 15C5(A)-phenol.

The red-shift of the S_1-S_0 electronic transition is generally observed in π-bound van der Waals complexes, such as phenol-Ar_n, benzene-Ar_n, and aniline-Ar_n, and their red-shifts become largest when one Ar atom is bound at each side of the aromatic ring (n=2)[12,13,14]. It is known that the interaction between the CH group and aromatic ring, conventional CH•••π interaction, is the dispersion force similar to the "π electrons•••rare gas atom" interaction, and the red-shifts of the S_1-S_0 electronic transitions are also observed in many clusters of methane-aromatic molecules[15,16]. Therefore, the S_1–S_0 electronic transition energy of 3nCn-phenol complexes can be red-shifted by interaction between the phenolic ring and the CH groups of the ethers. As seen in Figure 5(b), 15C5(II)-phenol has the two CH•••π bonds on both sides of the aromatic ring, showing the large red shift similar to the cases of phenol-Ar_2, benzene-Ar_2, and aniline-Ar_2.

From the calculated results, we understand that the unique stability of the 18C6-phenol structure results from the stability of the 18C6 conformation and effective intermolecular interactions constituted of O•••HO, CH•••π and O•••HC(aromatic). This collective intermolecular interaction is enhanced only when 18C6 forms a particular conformation. In the structure of the 18C6-phenol complex, the 18C6 cavity is matched to the shape of a phenol molecule like "**a lock (18C6) recognizes a key (phenol)**".

Experimental: Details of the experiment was described in our previous papers.[17,18] Briefly, jet-cooled CE-phenol complexes were generated by expanding a gaseous mixture of 3n-crown-n (12C4, 15C5, 18C6, or 24C8 heated at 40, 50, 80, 90 ºC, respectively), phenol, and helium (3 bar) into vacuum through a pulsed nozzle. For the generation of diethyl ether (DEE)-phenol or 1,4-dioxane (DO)-phenol complexes, liquid DEE or DO was put in a stainless steel bottle connected to a gas line. The partial pressure of DEE and DO was controlled by a thermo regulator. For the LIF

measurement, an output of a pulsed UV laser (Inrad, Autotracker III (BBO) / Lambda Physik, Scanmate / Continuum, Surelite II) was introduced to the vacuum chamber at ~30 mm downstream of the nozzle. LIF spectra were obtained by detecting the fluorescence as a function of UV frequency. In UV-UV HB spectroscopy, two UV lasers were used; pump and probe lasers. The frequency of the probe UV laser was fixed to a vibronic band of a specific species and its fluorescence signal was monitored. A pump UV laser (Inrad, Autotacker II (KDP)/ Continuum, ND6000/ Continuum, Surelite II) was introduced to the jet at ~10 mm upstream of the probe laser beam. The pump light was introduced ~4 μs prior to the probe one. When the pump laser frequency is resonant to a transition of the monitored species, the species is excited to the upper level, resulting in the depletion of the fluorescence signal monitored by the probe light. Thus, the electronic spectrum of the monitored species is obtained as a fluorescence dip spectrum as a function of the pump UV frequency. The experimental scheme of IR-UV DR spectroscopy for measuring infrared spectra is similar to that of UV-UV HB spectroscopy. An output of a tunable IR laser (Laser Vision/ Quanta-Ray, GCR250) was introduced coaxially with the UV probe laser with its frequency fixed to a vibronic band. The IR laser was irradiated at ~100 ns prior to the probe UV. The frequency of the IR pump laser was scanned while monitoring the fluorescence signal. The depletion of the fluorescence occurs when the IR frequency is resonant to vibrational transitions of the monitored species. Thus, IR spectrum in the S_0 state is obtained as a fluorescence dip spectrum.

Computational: For a broad structural survey of the isomers for the 3*n*C*n*-phenol complexes, we first carried out Monte Carlo simulation by mixed torsional search with low-mode sampling[19] in MacroModel V.9.1[20] with MMFF94s force field,[21] and optimized the geometries by PRCG algorithm with a convergence threshold of 0.05 kJ/mol. In order to eliminate redundant conformations from the optimized geometries, the maximum distance threshold was set to 0.5 Å. From this calculation, 300-1000 isomers for each 3*n*C*n*-phenol complex were obtained within 20 kJ/mol energy. All the isomers were optimized by density functional theory (DFT) calculation at M05-2X/6-31+G* level with *loose* optimization criteria using GAUSSIAN 09 program package.[22]

The 20 low-lying isomers were re-optimized for each complex at ωB97X-D/6-31++G** level with *tight* optimization criteria and *ultrafine* grid. The total energy was corrected by non-scaled zero-point vibrational energy (ZPE). The intermolecular interaction energy was computed without ZPE correction as:

$$E_{int}(\text{CE-phenol}) = E(\text{CE-phenol}) - E(\text{CE}) - E(\text{phenol}), \quad (1)$$

where the geometries of CE and phenol fragments are the same as those in CE-phenol complexes.

Acknowledgements

R.K. is supported by JSPS Research Fellowships for Young Scientists. T. E. acknowledges support from the Ministry of Education, Culture, Sports, Science, and Technology (MEXT) through a Grant-in-Aid for the Scientific Research on Priority Area "Molecular Science for Supra Functional Systems" (No. 477). Y. I. thanks the support of the JSPS through a Grant-in-Aid (No. 21350016).

Author information

Corresponding author

*E-mail : tebata@hiroshima-u.ac.jp

References

(1) Pedersen, C. J. Cyclic Polyethers and their Complexes with Metal Salts. *J. Am. Chem. Soc.* **1967**, *89*, 7017-7036.

(2) Pedersen, C. J. The Discovery of Crown Ethers. *Science* **1988**, *241*, 536-540.

(3) Steed, J. W; Atwood, J. L. *Supramolecular Chemistry – 2nd ed.*, John Wiley & Sons, Ltd., West Sussex, UK.

(4) Kusaka, R.; Kokubu, S.; Inokuchi, Y.; Haino, Y.; Ebata, T. Structure of Host-Guest Complexes between Dibenzo-18-crown-6 and Water, Ammonia, Methanol, and Acetylene: Evidence of Molecular Recognition on the Complexation. *Phys. Chem. Chem. Phys.* **2011**, *13*, 6827-6836.

(5) Kusaka, R.; Inokuchi, Y.; Ebata, T. Water-Mediated Conformer Optimization in Benzo-18-crown-6-ether/Water System. *Phys. Chem. Chem. Phys.* **2009**, *11*, 9132-9140.

(6) Watanabe, T.; Ebata, T.; Tanabe, S.; Mikami, N. Size-Selected Vibrational Spectra of Phenol-$(H_2O)_n$ (n = 1 - 4) Clusters Observed by IR-UV Double Resonance and Stimulated Raman- UV Double Resonance Spectroscopies. *J. Chem. Phys.* **1996**, *105*, 408-419.

(7) Ebata, T.; Watanabe, T.; Mikami, N. Evidence for the Cyclic Form of Phenol Trimer : Vibrational Spectroscopy of the OH Stretching Vibrations of Jet-Cooled Phenol Dimer and Trimer. *J. Phys. Chem.* **1995**, *99*, 5761-5764.

(8) Abe, H.; Mikami, N.; Ito, M. Fluorescence Excitation Spectra of Hydrogen-bonded Phenols in Supersonic Free Jet. *J. Phys. Chem.* **1982**, *86*, 1768-1771.

(9) Robertson, W.H.; Price, E. A.; J. M. Weber, J. M.; Shin, J. -W.; Weddle, G. H.; Johnson, M. A. Infrared Signatures of a Water Molecule Attached to Triatomic Domains of Molecular Anions: Evolution of the H-Bonding Configuration with Domain Length. *J. Phys. Chem. A* **2003**, *107*, 6527-6532.

(10) Myshakin, E. M.; Jordan, K. D.; Sibert III, E. L.; Johnson, M. A. Large Anharmonic Effects in the Infrared Spectra of the Symmetrical $CH_3NO_2^-(H_2O)$ and $CH_3CO_2^-(H_2O)$ Complexes. *J. Chem. Phys.* **2003**, *119*, 10138-10145.

(11) Iwasaki, A.; Fujii, A.; Watanabe, T.; Ebata, T.; Mikami, N. Infrared Spectroscopy of Hydrogen-Bonded Phenol-Amine Clusters in Supersonic Jets. *J. Phys. Chem.* **1996**, *100*, 16053-16057.

(12) Armentano, A.; Černý, J.; Riese, M.; Taherkhani, M.; Yezzar, M. B.; Müller-Dethlefs, K. Spectral Shifts and Structures of Phenol•••Ar_n Clusters. *Phys. Chem. Chem. Phys.* **2011**, *13*, 6077-6084.

(13) Schmidt, M. ; Mons, M.; Calvé, J. L. Characterization of Two Distinct One-Sided Isomers in the Benzene-Ar_3 Heterocluster: Influence of Microsolvation Symmetry on the Resonant Two-Photon Ionization Process. *J. Phys. Chem.* **1992**, *96*, 2404-2406.

(14) Douin, S.; Parneix, P.; Amar, F. G. ; Brechignac, P. Structure, Dynamics, and Spectroscopy of Aniline-$(Argon)_n$ Clusters. 1. Experimental Spectra and Interpretation for n=1-6. *J. Phys. Chem. A* **1997**, *101*, 122.

(15) Morita, S. ; Fujii, A.; Mikami, N. ; Tsuzuki, S. Origin of the Attraction in Aliphatic C−H/π Interactions: Infrared Spectroscopic and Theoretical Characterization of Gas-Phase Clusters of Aromatics with Methane *J. Phys. Chem. A* **2006**, *110*, 10583-10590.

(16) Tsuzuki S. ; Fujii, A. Nature and Physical Origin of CH/π Interaction: Significant Difference from Conventional Hydrogen Bonds. *Phys. Chem. Chem. Phys.* **2008**, *10*, 2584-2594.

(17) Ebata, T.; Hashimoto, T.; Ito, T.; Inokuchi, Y. ; Altunsu, F. ; Brutschy, B. ; Tarakeshwar, P. Hydration Profiles of Aromatic Amino Acids: Conformations and Vibrations of *L*-Phenylalanine-$(H_2O)_n$ Clusters. *Phys. Chem. Chem. Phys.* **2006**, *8*, 4783-4791.

(18) Inokuchi, Y.; Kobayashi, Y.; Ito, T.; Ebata, T. Conformation of *L*-tyrosine Studied by Fluorescence-Detected UV-UV and IR-UV Double-Resonance Spectroscopy. *J. Phys. Chem. A* **2007**, *111*, 3209-3215.

(19) Kolossváry, I.; Guida, W. C. Low Mode Search. An Efficient, Automated Computational Method for Conformational Analysis: Application to Cyclic and Acyclic Alkanes and Cyclic Peptides. *J. Am. Chem. Soc.* **1996**, *118*, 5011-5019.

(20) MacroModel, version 9.1, Schrödinger, LLC, New York, NY, 2005.

(21) Halgren, T. A. MMFF VII. Characterization of MMFF94, MMFF94s, and Other Widely Available Force Fields for Conformational Energies and for Intermolecular-Interaction Energies and Geometries *J. Comput. Chem.* **1999**, *20*, 730-748.

(22) Frisch, M. J.; Trucks, G. W.; Schlegel, H. B.; Scuseria, G. E.; Robb, M. A.; Cheeseman, J. R.; Scalmani, G.; Barone, V.; Mennucci, B.; Petersson, G. A. *et al.* Gaussian 09, revision A.02; Gaussian, Inc.: Wallingford, CT, **2009**